ARTICLE

A perfusion chamber for monitoring transepithelial NaCl transport in an in vitro model of the renal tubule

Jose Yeste[1,2,3] (iD) | Laura Martínez-Gimeno[4] | Xavi Illa[1,2] | Pablo Laborda[4] | Anton Guimerà[1,2] | Juan P. Sánchez-Marín[4] | Rosa Villa[1,2] | Ignacio Giménez[4,5]

[1] Institut de Microelectrònica de Barcelona, IMB-CNM (CSIC)., 08193, Bellaterra, Barcelona, Spain

[2] CIBER-BBN, Networking Center on Bioengineering, Biomaterials and Nanomedicine, Barcelona, Spain

[3] Departamento de Microelectrónica y Sistemas Electrónicos, Universitat Autònoma de Barcelona, Spain

[4] Instituto Aragonés de Ciencias de la Salud, IIS Aragón, Zaragoza, Spain

[5] Universidad de Zaragoza, Zaragoza, Spain

Correspondence
Jose Yeste, Institut de Microelectrònica de Barcelona, IMB-CNM (CSIC) 08193, Bellaterra, Barcelona, Spain.
Email: jose.yeste@csic.es

Abstract

Transepithelial electrical measurements in the renal tubule have provided a better understanding of how kidney regulates electrolyte and water homeostasis through the reabsorption of molecules and ions (e.g., H_2O and NaCl). While experiments and measurement techniques using native tissue are difficult to prepare and to reproduce, cell cultures conducted largely with the Ussing chamber lack the effect of fluid shear stress which is a key physiological stimulus in the renal tubule. To overcome these limitations, we present a modular perfusion chamber for long-term culture of renal epithelial cells under flow that allows the continuous and simultaneous monitoring of both transepithelial electrical parameters and transepithelial NaCl transport. The latter is obtained from electrical conductivity measurements since Na^+ and Cl^- are the ions that contribute most to the electrical conductivity of a standard physiological solution. The system was validated with epithelial monolayers of raTAL and NRK-52E cells that were characterized electrophysiologically for 5 days under different flow conditions (i.e., apical perfusion, basal, or both). In addition, apical to basal chemical gradients of NaCl (140/70 and 70/140 mM) were imposed in order to demonstrate the feasibility of this methodology for quantifying and monitoring in real time the transepithelial reabsorption of NaCl, which is a primary function of the renal tubule.

KEYWORDS
cell layer capacitance, microfluidic cell culture, renal epithelium, sodium reabsorption, transepithelial electrical resistance, transepithelial ion fluxes

1 | INTRODUCTION

Transepithelial electrical measurements of the renal tubule—carried out by in vivo micropuncture (Lorenz, 2012), ex vivo isolated microperfused tubule (Burg & Green, 1973; Muto et al., 2010; Stockand, Vallon, & Ortiz, 2012), or in vitro cell culture (Furuse, Furuse, Sasaki, & Tsukita, 2001)—have provided a better understanding of the renal function and its reabsorption capacity. Although the best methodology is to use native tissue, these experiments and measurement techniques have poor reproducibility and are time-limited, and difficult to prepare. In addition, the size and architecture of the renal tubule has made difficult to apply in vitro tools, like the versatile Ussing chamber (Li, Sheppard, & Hug, 2004; Ussing & Zerahn, 1951) that has been instrumental in understanding function of other epithelia (e.g., intestinal or placental epithelia), to excised tubules. For these reasons and also due to ethical issues of animal testing, in vitro research for polarized renal epithelium has been limited to studies on Transwell devices (Terryn et al., 2007; Yu, Enck, Lencer, & Schneeberger, 2003). Nowadays microfluidic cell cultures

have become more popular as cells can be exposed to fluid shear stress (FSS) (Ferrell, Ricci, Groszek, Marmerstein, & Fissell, 2012; Ha, Jang, & Suh, 2014; Jang et al., 2013), which is an important physiological stimulus for renal epithelial cells (Weinbaum, Duan, Satlin, Wang, & Weinstein, 2010). Nevertheless, the integration of electrodes within these microphysiological systems is an important issue that can impair the uniform current distribution required for transepithelial measurements (Yeste et al., 2016). Sensing capabilities in these microphysiological systems, similar to those of the Ussing chamber, will be useful to study the renal function in a more physiological microenvironment.

Transepithelial electrical measurements offer a non-destructive, label free, and easily applicable technique to measure the electrical properties of epithelial tissues in real time. In particular, transepithelial electrical resistance (TEER) provides information about the ion conductive pathways and is often used to ensure cell barrier integrity during experiments. TEER is the parallel of the paracellular (between cells) and transcellular (through cells) resistances. In "leaky" epithelia, the paracellular resistance is much lower than the transcellular one, whereas, it is similar or higher in "tight" epithelia (FröMter & Diamond, 1972). In addition to the TEER, the cell layer capacitance (C_{cl}) can be also obtained by means of electrical impedance spectroscopy (EIS) (Benson, Cramer, & Galla, 2013; Clausen, Lewis, & Diamond, 1979), which can yield information about the membrane surface area and how much it is folded since the capacitance of unfolded biological membranes is relatively constant around $1\,\mu F\,cm^{-2}$ (Cole, 1972). This parameter serves to identify the formation of complex surface morphologies such as microvilli structures (Wang et al., 1994; Wegener, Abrams, Willenbrink, Galla, & Janshoff, 2004). Some authors have developed microfluidic systems with integrated electrodes (Brakeman et al., 2016; Ferrell et al., 2010) or also organic electrochemical transistors (Curto et al., 2017) for the evaluation of renal epithelial cells under flow.

Renal epithelial cells are localized in the nephron. This is the functional unit of the kidney and regulates electrolyte and water homeostasis by filtering the blood, reabsorbing solutes, and excreting waste products. Reabsorption takes place in the renal tubule, which is divided into proximal tubule (PT), loop of Henle, and distal nephron (comprising the distal convoluted tubule [DCT], connecting tubule, and collecting ducts). Each segment exhibits different absorptive capabilities and is exposed to particular electrochemical gradients across epithelium. For example, the PT reabsorbs the 65% of the filtered Na^+, whereas the thick ascending limb (TAL) segment of the loop of Henle and the DCT reabsorb the 25% and the 5%, respectively (Greger, 2000). Na^+ and Cl^- are reabsorbed in the renal tubule from the luminal space to the peritubular capillaries. As a result, much of these ions return from the filtrate to the bloodstream instead of being excreted. Renal epithelial cells manage this reabsorption. Transepithelial reabsorption can be mediated by active transport through the transcellular route moving ions and molecules up its electrochemical gradients or also by passive diffusion, in which the solutes could be moved down its electrochemical gradient in either route. In the paracellular pathway, tight junctions govern the passive diffusion by sealing the intercellular space.

An important mechanical stimulus for renal epithelial cells is FSS. In tubular epithelial cells cultured in vitro, physiological levels of FSS

alters cytoskeletal organization and transport proteins resulting in enhanced epithelial cell phenotype (Duan, Weinstein, Weinbaum, & Wang, 2010; Mohammed et al., 2017; Raghavan, Rbaibi, Pastor-Soler, Carattino, & Weisz, 2014). On the other hand, pathological levels of FSS may be responsible for losing of epithelial characteristics that may account for the progression of chronic kidney disease (Grabias & Konstantopoulos, 2014; Maggiorani et al., 2015).

In previous work, we developed a chamber system with integrated electrodes to perform impedance analysis of epithelial or endothelial cell monolayers (Yeste, Illa, Guimerà, & Villa, 2015). As a novelty, we present a similar system for long-term culture of renal epithelial cells under flow that allows—using the same electrodes—the continuous and simultaneous monitoring of transepithelial electrical parameters and transepithelial NaCl transport. Since Na^+ and Cl^- are the ions that contribute most to the electrical conductivity of a standard physiological solution, their concentration can be estimated from the conductivity. Therefore, it is possible to determine the transport of NaCl by measuring the electrical conductivity in the apical and basal compartments. In the present study, we have electrophysiologically characterized in the perfusion chamber epithelial monolayers obtained with two rat cell lines representing the PT (NRK-52E) and TAL (raTAL) segments in the nephron. This in vitro model of the renal tubule was used to validate the measurement system capable to measure the TEER, the C_{cl}, and the conductivity of apical and basal compartments. For that purpose, an apical to basal gradient of NaCl in both epithelial monolayers was imposed in order to follow the transport of NaCl. In this way, it is possible to monitor in real time the transcellular chemical gradient of NaCl either imposed or produced by active transporters.

2 | MATERIALS AND METHODS

2.1 | Perfusion chamber design and fabrication

The custom-made perfusion chamber is similar to that described in Yeste et al.(2015). The device is composed of two plates and a disposable membrane with three cell culture areas of 0.8 cm^2 (4 × 20 mm) (Figures 1a and 1b). Plates were completely made of cyclo-olefin polymer (COP) (Zeonor 1420R, Microfluidic ChipShop GmbH, Jena, DE) and had integrated electrodes to perform EIS. Pads of the electrodes were soldered to electric wires and covered with epoxy. Fluid inlets and outlets were defined in the plates using a CNC milling machine (MDX-40A, Roland Digital Group Iberia, S.L., Cerdanyola del Vallès, ES).

Polyethylene terephthalate (PET) porous membranes of 0.4 μm of pore size (ipCELLCULTURE membranes, it4ip SA, BE) and polycarbonate (PC) porous membranes of 1 μm of pore size (Whatman Cyclopore, GE Healthcare Europe GmbH, Barcelona, ES) were modified to be integrated into the perfusion chamber. Two silicone sheets (platinum cured sheet, Silex Ltd., UK) of 0.5 mm in thickness were cut using a cutting plotter and bonded to both sides of the membrane using double-side pressure-sensitive adhesive (PSA) (ARcare 8939, Adhesives Research Ireland Ltd., Limerick, IE). These silicone sheets were used to define the apical and basal compartments (5 × 25 mm in area), both resulting in a total height of 0.7 mm (silicone plus PSA and COP) and a
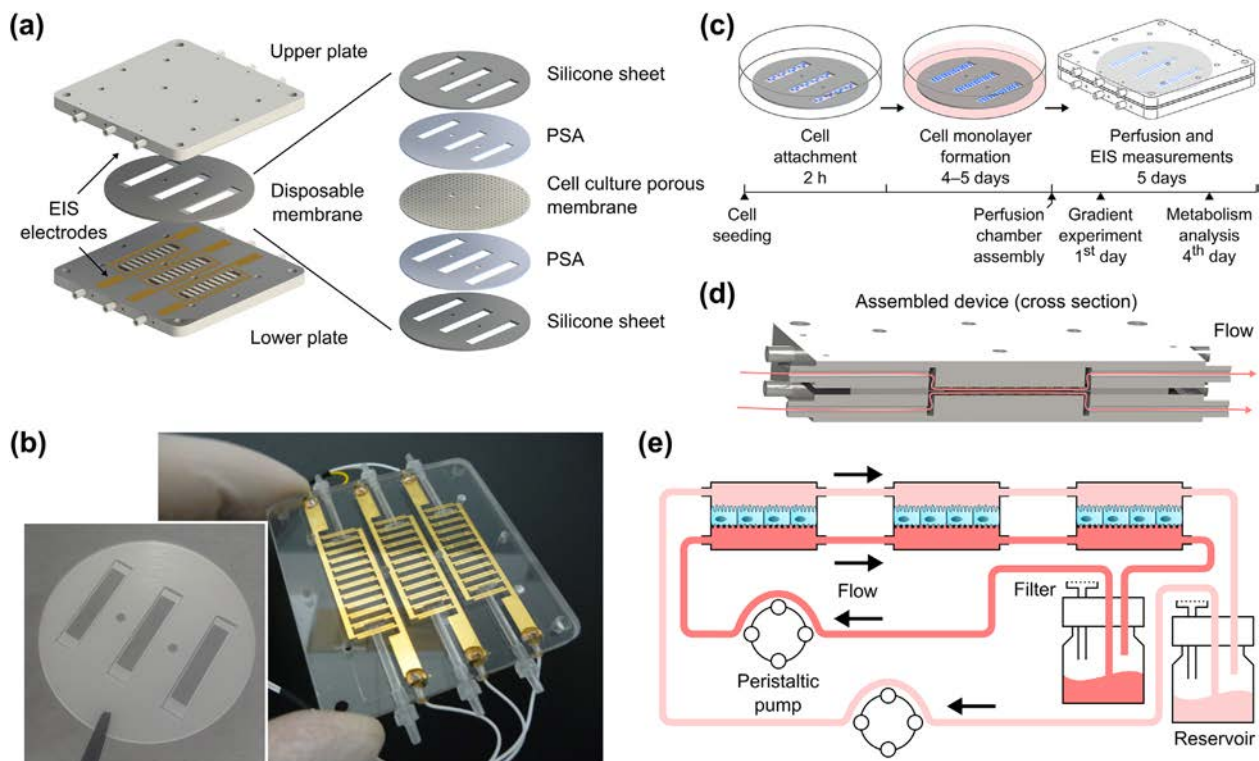
FIGURE 1 Perfusion chamber assembling and experimental set-up. (a) Assembling parts of the system including upper plate, lower plate, and disposable membrane. There is also included a schematic decomposition of the disposable membrane fabrication. This is formed through a stack of layers consisted of two silicone sheets (0.5 mm in thickness), two double-sided PSA layers, and a tissue-culture treated polyethylene terephthalate (PET) porous membrane of 0.4 µm of pore size and 10 µm in thickness. (b) Pictures of the disposable membrane and a plate. Note that upper and lower plates are identical. (c) Experimental set-up procedure including cell seeding and attachment on the membrane (2 hr), cell proliferation (4–5 days), and perfusion chamber assembly. (d) Cross-section of the assembled device with detail (pink arrows) of flow paths. (e) Schematic representation of the fluidic system. Two identical fluidic circuits were mounted to control independently the apical and basal flow. The three apical or basal compartments were connected in series with silicone tubing, and the circuit was closed through a reservoir and a peristaltic pump. EIS, electrical impedance spectroscopy; PSA, pressure-sensitive adhesive

volume of ~87 µl. The final assembly of the device was made by sandwiching the modified membrane between the plates and, in turn, between two steel plates that were screwed together to keep the system fluidically sealed. Altogether, the perfusion chamber comprises three replicas of a double compartment system separated by a porous membrane and with independent electrodes; therefore, three experiments can be performed simultaneously.

2.2 | Cell culture

Epithelial monolayers were obtained with two immortalized rat cell lines representing PT (NRK-52E, ATCC, Manassas, VA) and TAL (raTAL; donation from N. Ferreri, New York Medical College Valhalla, NY, Eng et al., 2007) phenotypes. Both cell lines were adapted to grow on low-serum culture medium supplemented with insulin (5 µg ml^{-1}), transferrin (5 µg ml^{-1}), sodium selenite (60 nM), dexamethasone (0.05 µM), triiodothyronine (1 nM), and epidermal growth factor 10 (ng ml^{-1}) (Sigma–Aldrich, Quimica SL, Madrid, ES), specifically tailored to meet renal epithelial cell needs (Taub & Sato, 1980). The device culture membrane was sterilized by exposure to UV light for 30 min on each side, and the rest of the system was sterilized by autoclave at 121 °C for 15 min. Prior

to cell seeding, membrane was coated with collagen type I (0.4 mg ml^{-1}, 50 µg cm^{-2} (100 µl per channel) in phosphate-buffered saline (PBS), incubated at 37 °C for 1 hr, and rinsed three times with PBS. Cells were seeded on each culture area of the membrane at a concentration of ~40.000 cells per channel in 300 µl complete culture medium and maintained inside a Petri dish for 2 hr until cell attachment. In experiments involving both cell lines, NRK-52E cells were seeded on one of the three cell culture areas of the membrane, while raTAL cells were seeded on the other two ones. Then, unattached cells were carefully aspirated, and the Petri dish was filled with culture medium and maintained at 37 °C and 5% CO$_2$, refreshing culture medium every 2–3 days. Cells typically reached confluence after 2 days. On coverslips, cells formed an efficient barrier at the 3rd day post-confluence as revealed by ZO-1 expression (Figure S4). On day 4–5, membrane and plates were assembled to expose the cells to flow perfusion and to perform EIS (Figures 1c and 1d).

Epithelial monolayers were confirmed by means of phase-contrast microscopy and a Ca^{2+} switch protocol. In the latter procedure, the culture medium in the chamber was replaced with medium containing 1 mM of ethylenediaminetetraacetic acid (EDTA) and without CaCl$_2$. After maintaining the cells under these conditions for 12 min, the

medium in the chamber was returned to the normal culture medium that includes 1 mM of CaCl$_2$.

2.3 | Fluidic set-up and experimental design

Compartments of the device were fluidically connected using silicone tubing (0.8 mm in internal diameter [ID] and 2.4 mm in outer diameter [OD]) as depicted in Figure 1E. Apical and basal compartments were perfused with independent fluidic circuits using two reservoirs and a peristaltic pump (Reglo ICC, Cole-Parmer GmbH, Wertheim, DE). The volume of the culture medium for apical and basal circuits was replaced every 4 days (10 ml for each). Three-way stopcocks were placed at the inlets and outlets of each compartment to provide a way to collect samples after experiments with static conditions. Culture medium samples from the reservoir or collected from the compartments were analyzed for glucose, lactate, and ion concentrations using an automated analyzer (AU680 Chemistry Analyzer, Beckman Coulter Inc., Brea, CA).

After assembling the membrane in the device, cells were apically and basally perfused with culture medium at a flow rate of 0.2 ml min^{-1} (FSS of 0.07 dyn cm^{-2}, Figures S1A and S1B) during 1 day to stabilize the cells exposed to flow before each experiment. Apical and basal fluids were flowed in the same direction, and effluxes were recirculated. With this fluidic set-up, the NaCl chemical gradient is expected to reach a steady state in which the NaCl absorption (apical to basal) is equal to the NaCl backflow (basal to apical).

2.4 | Imposed transepithelial NaCl chemical gradient

To validate the measurement system to provide an estimate of NaCl concentration, an experiment was performed imposing different apical to basal chemical gradients for Na$^+$ and Cl$^-$. This strategy allowed us to aess the transepithelial ion transport as well as to monitor the transepithelial electrical parameters under different ion gradients. First, culture mediums were replaced by Ringer's solutions and left for stabilization for 1 to 2 hr. Standard Ringer's solution was composed of (in mM) 140 NaCl, 4 KCl, 1 MgCl$_2$, 1 CaCl$_2$, 5 Glucose, 10 Hepes, and pH 7.4. Then, one of the solutions bathing the apical or basal compartments was replaced by a modified Ringer's solution containing 70 mM of NaCl (substituted isoosmotically with N-Methyl-Glucamine (NMG)/gluconate), and flow was stopped to avoid any further diffusion from the compartments. Meanwhile, the opposite compartment was still perfused with standard Ringer's solution (140 mM NaCl). All solutions were allowed to equilibrate to incubator conditions before being used in the fluidic circuit.

2.5 | Electrical conducvity and ionic species

The electrical conductivity (k) of an electrolyte solution is given by

$$k = \Lambda_m c, \tag{1}$$

where Λ_m is the molar conductivity and c is the molar concentration (Robbins, 1972). According to the Kohlrausch's law of independent migration of ions, each ionic species contributes to the conductivity

independently of other ions, particularly at infinite dilution ($c \to 0$). Then, Λ_m can be defined as the sum of all ionic conductivities:

$$\Lambda_m = \Sigma_i \lambda_i \tag{2}$$

in which λ_i is the ionic conductivity of a particular species i. Since ions contribute differently to the overall conductivity, it is interesting to quantify the particular contribution of each ion. The fraction of the conductivity of a given ion i is called its transport number (t_i), and it is calculated as

$$t_i = \frac{c_i \lambda_i}{\sum_i c_i \lambda_i}, \tag{3}$$

where c_i is the molar concentration of i-ions. For strong electrolytes where solutes almost completely dissociates in solution, λ_i is equal to the limiting molar conductivity (λ_i^0) at infinite dilution and decreases linearly with the square root of the concentration. Contributions of each compound in the Ringer's solution to the conductivity are shown as supplementary information in Table S1 for the approximation of infinite dilution. Although there are several salts in the solution, conductivity is dominated by the NaCl pair due to the high difference in concentrations. This is evidenced by a t_{NaCl} close to 1 and a t_i close to 0 for the rest ($t_{\text{NaCl}} = 0.94$ (140 mM NaCl); $t_{\text{NaCl}} = 0.89$ (70 mM NaCl); $t_{\text{NaCl}} = 0.66$ (70 mM NaCl + 70 mM NMG-gluconate)). In this scenario, it is possible to estimate NaCl concentration from conductivity measurements, especially if the concentrations of the other salts remain constant.

The electrical conductivity of an electrolyte solution can be measured using a pair of electrodes exposed to the solution according to the following equation:

$$k = K_{\text{cell}} \, G, \tag{4}$$

where G is the electrical conductance measured between the pair of electrodes and K_{cell} is the cell constant, which depends of the geometry of the electrodes. This methodology is simple and fast, and many commercially available conductivity meters employ this principle to measure the k of electrolytic solutions (e.g., EC-Meter GLP 31, Crison Instruments SA, Barcelona, ES).

2.6 | Impedance analysis

We managed to measure simultaneously transepithelial electrical parameters and solution conductances by changing the electrical connections between the device and an impedance analyzer (Guimerà, Gabriel, Parramon, Calderón, & Villa, 2009). This switching was performed automatically with a custom-made relay multiplexer device. Both electrical connections are shown in Figure 2.

Impedance measurements across an epithelial monolayer can be interpreted in terms of its electrical properties by the equivalent electric circuit shown in Figure 2a. This is a simplified model with lumped elements and consists of the resistance of the medium solution (including the medium resistance through the pores of the
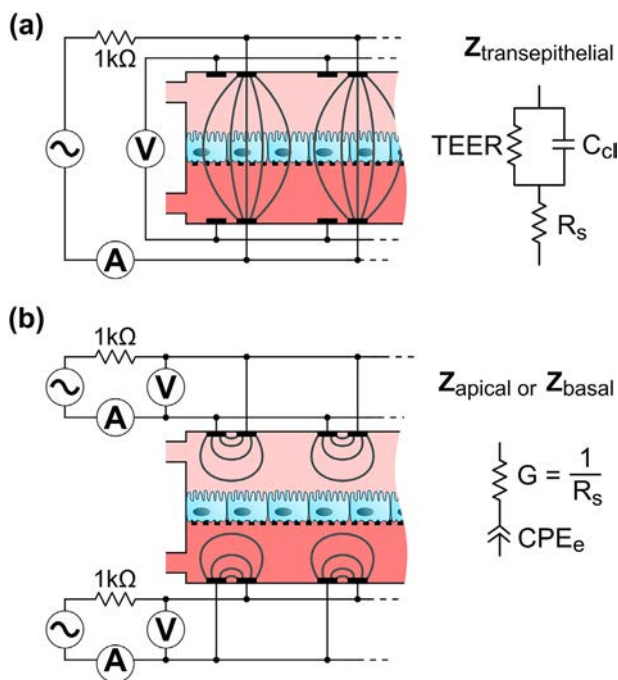
FIGURE 2 Schematic representation of the measurement system. Electrical connections between the device and the impedance analyzer for measuring (a) transepithelial electrical impedance, (b) apical conductance, and basal conductance. There are included the equivalent electric circuits with lumped elements. For transepithelial impedance, this consists in the resistance of the medium solution (R_s) in series with the parallel of TEER and C_{cl}. For apical and basal impedances, this consists of the conductance of the medium solution (G) in series with a constant phase element that represents the electrode polarization impedances (CPE_e). Note that it is not drawn to scale and is a section of the perfusion chamber. The resistance of 1 kΩ in series with the sine wave generator limits the maximum current applied to the cells, so the maximum applied voltage and current are 10 mV and 10 μA, respectively. V, voltmeter; A, ammeter; ∼, sine wave voltage perturbations at different frequencies

semipermeable membrane) (R_s) in series with the parallel of TEER and C_{cl}. These parameters were obtained by impedance analysis using EIS. Impedance spectra were measured at 20 frequencies, ranging from 10 Hz to 1 MHz, and each measurement was fitted to the equivalent electric circuit using the least-squares method in Matlab. For measuring apical or basal conductances, impedances were measured between the two apical (in the upper plate) or the two basal (in the lower plate) interdigitated electrodes, respectively. Then, impedance data was fitted to the equivalent electric circuit consisting of the conductance of the medium solution (G) in series with a constant phase element representing the electrode polarization impedances (CPE_e) (Figure 2b).

3 | RESULTS AND DISCUSSION

3.1 | Electrophysiological characterization of cells during long-term culture under flow

We experimentally validated the fabricated chamber system to electrophysiologically characterize renal cell monolayers under

perfusion. First, we optimized the conditions for achieving rapid formation of a confluent cell monolayer. PET and PC porous membranes were evaluated as a support for forming NRK-52E and raTAL cell monolayer. Phase-contrast images of both cell types on PC or PET membranes are shown in Figure 3a. Cells growing on PET membrane reached confluence after 2 days and showed good standing of perfusion in the device. Otherwise, cells on PC membrane were able to attach and spread but not to fully proliferate on the whole membrane. Thus, best conditions were shown to be seeding NRK-52E or raTAL cells at high density on collagen type I-coated PET membranes; the rest of the experiments were done under these conditions. Application of 0.2 ml min^{-1} flow rates to either one or both compartments supported long term survival (≥2 weeks) of both cell lines. With this flow rate, cells were subjected to a FSS of 0.07 dyn cm^{-2}. Although this FSS may not be physiologically relevant (the in vivo value is approximately 0.2 dyn cm^{-2}), perfusion served to continuously supply the cells with nutrients and gases (i.e., O_2 and CO_2) as well as to take away the waste.

Real-time, continuous TEER recording was used to assess cell monolayer health during long-term culture. To confirm the formation of both epithelial monolayers and to demonstrate that TEER values were dependent on tight junction paracellular resistance, we performed a Ca^{2+} switch protocol. This is a well-established method relying in the calcium-dependency of tight junction formation so that monolayers cultured in a low Ca^{2+} medium lack barrier formation (Gonzalez-Mariscal et al., 1990). During a Ca^{2+} switch (transition from a Ca^{2+} depleted medium to a normal Ca^{2+} medium), tight junctions reassemble in few hours. The time course of the TEER during a reduction and subsequent recovery of the Ca^{2+} concentration is shown in Figure 3b. TEER values of both NRK-52E and raTAL cells fell and rose according to Ca^{2+} reduction and recovery, respectively. Epithelial monolayer formed with NRK-52E cells exhibited a TEER of 9.1 ± 0.4 Ω cm^2 and a C_{cl} of 0.50 ± 0.04 μF cm^{-2} after being perfused for 1 day, while they were 600 ± 80 Ω cm^2 and 1.56 ± 0.14 μF cm^{-2} for raTAL cells. Impedance spectra measured through both cell layers (Figures S2A and S2B) and time course of TEER and C_{cl} in raTAL cells under different flow conditions (Figure S3) are shown as supplementary information. Flow in the basal compartment not only supplies cells with continuous nutrients at the basolateral side, as occurs in vivo, but also helps to remove the waste and to maintain a constant concentration of solutes—an issue that most microfluidic cell cultures fail to reproduce.

Samples of medium perfusate were analyzed to determine several metabolic parameters. The metabolism of raTAL cells is summarized in Table 1. Surprisingly, data shows that cells have polarized energy metabolism toward the apical site (preferred site to uptake glucose and dump lactate), the opposite to what could be expected in vivo in the original tissue. Although we cannot confirm the origin of this abnormal polarization, this could be because continuous cell lines have been selected to thrive in 2D culture, where all metabolic exchange takes place through the apical membrane. Interestingly, we were able to detect Na^+ reabsorption in the perfusion chamber. There was a significant difference of Na^+ concentration; the concentration in the
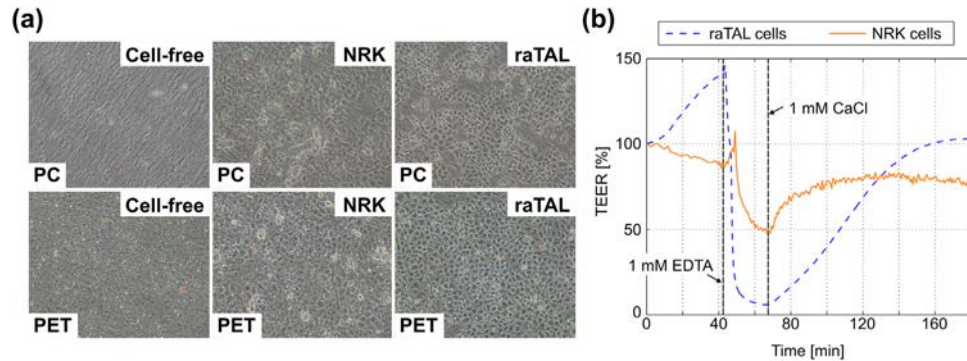
FIGURE 3 (a) Phase-contrast images of NRK-52E and raTAL cells growing on PC or PET membranes for TEER device. Cells were seeded at high density in 300 μl per channel and allowed to attach for 2 hr before filling the dish with culture medium. Cells growing on PET reached confluence after 2 days and showed good standing of perfusion in the device. (b) Time course of the TEER during a Ca^{2+} switch protocol for raTAL (blue dashed line) and NRK-52E (orange line) cells. Arrows point the time of Ca^{2+} removal plus the administration of 1 mM of ethylenediaminetetraacetic acid (EDTA) and Ca^{2+} recovery plus EDTA removal. PC, polycarbonate; PET, Polyethylene terephthalate

apical side was ~5 mM lower than in the basal side (~4 mM for Cl^-). This gradient, measured after 4 days in the perfusion chamber, corresponds to a net transport of NaCl of ~0.15 nmol cm^{-2} s^{-1}. Despite this is much lower than the transport in isolated perfused TAL segments (1–10 nmol cm^{-2} s^{-1}; rat, mouse, and rabbit) (Burg, 1982), it proves the existence of active mechanisms of Na^+ transport. The TAL is known as the diluting segment because it is able to reduce luminal NaCl concentrations up to 30 mM. This is achieved through the combination of active NaCl transepithelial transport and a very tight barrier that is water impermeable. Our findings confirm the high barrier formed by raTAL, but the magnitude of NaCl transport does not appear to be similar to that observed in vivo, most likely because we could not demonstrate expression of the major protein responsible for active transport (NKCC2) in these cells. In any case, this example illustrates the validity of the system to readily acquire valuable information about the renal epithelium health and function. Metabolic rates did not change significantly over the course of long-term culture.

Electrical conductance and NaCl concentration Renal epithelium in vitro should reproduce the in vivo function, which basically consists in reabsorbing large quantities of solutes and ions. Differences in ion selectivity and water permeability induce the formation of electrochemical transepithelial gradients, especially in the TAL. That prompted us to propose using a different configuration of the TEER electrodes to

TABLE 1 Metabolism of raTAL cells cultured in the device

	Basal	Apical
Glucose flux (μmol h^{-1} cm^{-2})	0.054 ± 0.04	0.092 ± 0.051
Lactate flux (μmol h^{-1} cm^{-2})	0.048 ± 0.031*	0.100 ± 0.055*
$[Na^+]_o$ (mM)	152.3 ± 5.9*	147.5 ± 4.6*
$[K^+]_o$ (mM)	4.08 ± 0.82	4.44 ± 0.56
$[Cl^-]_o$ (mM)	141.9 ± 9.9	138.2 ± 8.2

These values were analyzed from samples collected at the reservoirs after the cells were perfused in the bioreactor for 4 days (*$p < 0.05$ by unpaired student's t-test) ($n = 3$).

determine medium conductance in both compartments (corresponding to apical and basolateral cell poles) and, in turn, to estimate NaCl transport and its potential active transport across the epithelium. Electrical characterization of the measurement system using different NaCl concentrations is shown in Figure 4a. To avoid the systematic error due to slightly variations in the cell constant of the electrodes placed at each compartment, conductance was normalized to the value measured at 140 mM of NaCl. The relation between variation in the conductance and the concentration of NaCl were linear at least for values lower than 140 mM (Figure 4b). The maximum uncertainty in the percentage of conductance was ±0.93 %, which was equivalent to ±2.4 mM in the estimation of the NaCl. The measured Na^+ concentration gradient for raTAL cells cultured in the perfusion chamber was ~5 mM. As mentioned above, other ion species also influences conductance. In the range from 70 to 140 mM, the conductance of the Ringer's solution is dominated by the NaCl due to the high concentration and mobility of Na^+ and Cl^- against other ions.

3.2 | Transepithelial transport of NaCl

Since raTAL epithelium in the chamber system did not exhibit the large active NaCl transport characteristic of native TAL (only a 5 mM NaCl gradient), we designed an experiment (Figure 5a) to validate the conductance measurement system as a method to analyze the role of tight junctions in NaCl transepithelial transport in a renal cell monolayer. Instead of relying on active transport, artificial transepithelial NaCl gradients were imposed by replacing the medium in one of the compartments with an isoosmotic solution containing 70 mM NaCl, while keeping the opposite compartment in a standard Ringer's solution (140 mM NaCl). Thus, the electrochemical gradient lead to the movement of NaCl from the concentrated compartment toward the diluted one, whereas ion diffusion rates should be determined by the tightness of the epithelium.

Measurements of the conductance in both compartments allowed us to follow in real time the transepithelial transport of NaCl while measuring simultaneously transepithelial electrical parameters. Time
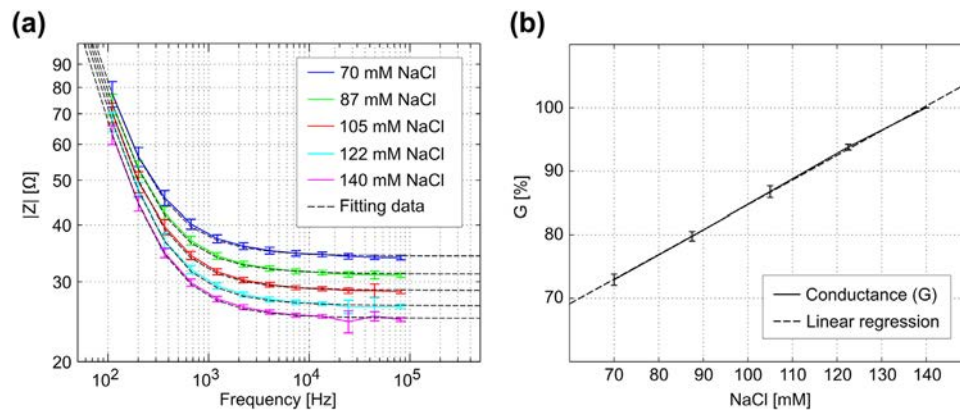
FIGURE 4 Electrical characterization of the estimation of NaCl through EIS. (a) Impedance spectra at different NaCl concentrations using a blank porous membrane. Chambers were filled with Ringer's solutions of 70 (blue line), 87.5 (green line), 105 (red line), 122.5 (cyan line), and 140 mM (magenta line) of NaCl, and impedance spectra were measured at 37 °C and 12 frequencies, ranging from 100 Hz to 100 kHz. The fitting data according to the equivalent electric circuit is shown in dashed line. (b) Variation in conductance as a function of the NaCl concentration (solid line) and linear regression line (dashed line) ($n = 6$). Data is normalized to the conductance measured at 140 mM of NaCl (100%)

course measurements of electrical conductance, NaCl concentration, TEER, and C_{cl} are shown in Figure 5 for epithelial monolayers obtained with NRK-52E and raTAL cells. Note that the y-axis of Figure 5b shows the NaCl concentration calculated through the linear regression line included in Figure 4b. Immediately after decreasing the NaCl concentration in basal (+ gradient experiment, apical NaCl > basal NaCl) or apical (− gradient experiment, apical NaCl < basal NaCl) compartments and stopping the flow, the recovery of NaCl concentration in the 70 mM compartment occurred driven by the electrochemical force between both comportments (Figure 5b). This rise was much faster for NRK-52E cells than for raTAL cells. NaCl concentrations of the 70 mM compartment at 1 and 2.5 hr are summarized in Figure 5c. In detail, NaCl concentrations after 2.5 hr were 138 (+Grad.) and 129 ± 2 mM (−Grad.) for NRK-52E cells, while concentration were 101 ± 7 (+Grad.) and 80 ± 5 mM (−Grad.) for raTAL cells. Otherwise, opposite compartments maintained 140 mM as expected from the continuous flow with the Ringer's solution (140 mM NaCl). Note that the porous membrane, where cells are cultured, partly contributes to maintain the concentration gradient. Therefore, there is a slow recovery of the gradient even with a very leaky epithelium, such as that formed by NRK-52E cells.

The metabolic values of the main ionic species in the solution are shown in Table 2. For both cell types, cells had again polarized energy metabolism toward the apical site. Furthermore, there was a significant difference for the Na$^+$ and Cl$^-$ concentration between NRK-52E and raTAL cells, which is in accordance with the results obtained by conductance measurements. However, such values were lower in the case of NRK-52E cells; it may be accounted for the medium contained in the tubes, which can be unbalanced with the medium in the compartment. This highlights the importance of in-line measurements since it is often difficult to collect samples from a specific place within microfluidic channels. In the PT, Na$^+$ is absorbed through the Na$^+$/H$^+$ exchanger (NHE3) and the Na$^+$/glucose cotransporter in the apical membrane cooperating with the

Na$^+$-K$^+$-ATPase and the Na$^+$/HCO$_3^-$ cotransporter in the basolateral membrane. Concurrently, most of the Cl$^-$ is reabsorbed paracellularly due to the generated electrochemical gradient, although Cl$^-$ channels and Cl$^-$-coupled transporters also contribute to Cl- reabsorption (Planelles, 2004). NRK-52E cell line is derived from PT and express Na$^+$/glucose cotransporter (Dong, Chen, He, Yang, & Zhang, 2009). The epithelium of PT has low transepithelial resistance and is considered a "leaky" epithelium, in which the paracellular resistance is much lower than the transcellular resistance. This means that paracellular pathway is very permeable to ions and a chemical gradient will tend to equalize rapidly, as it happened in our experiments. In vivo, the PT achieves to maintain the reabsorbed Na$^+$ by the drag of water and Cl$^-$ into the peritubular space because of osmosis and electrodiffusion, respectively; otherwise, Na+ would return to the filtrate (Palmer & Schnermann, 2015). On the other hand, raTAL cells were derived from the TAL—the initial segment in the distal nephron. In the TAL, the NaCl is transported into cells via the apical Na$^+$-K$^+$-2Cl$^-$ cotransporter (NKCC2), and Na$^+$ and Cl$^-$ are secreted into the basolateral side through the Na$^+$-K$^+$-ATPase pump and the chloride channel Kb (ClC-Kb)/barttin channel, respectively. Both transport proteins, required for Na$^+$ reabsorption (i.e., NKCC2 and Na$^+$-K$^+$-ATPase), have been detected in raTAL cells (Eng et al., 2007). TAL is a tight epithelium and impermeable to water, being among the tighter epithelia in the human body. In such epithelia, the value of the paracellular resistance may be similar to transcellular one. This is an important requirement to efficient transepithelial transport since a leaky paracellular pathway that would allow for ion backflow would dissipate the chemical energy accumulated as NaCl trans-epithelial gradient, which is achieved through a secondary active transport through ATP consumption. Differences between time courses for passive transepithelial NaCl transport in NRK-52E and raTAL cells are in good agreement with what is expected from PT and TAL epithelia. Moreover, the NaCl transport was faster during positive gradients than during negative gradients for both cells.
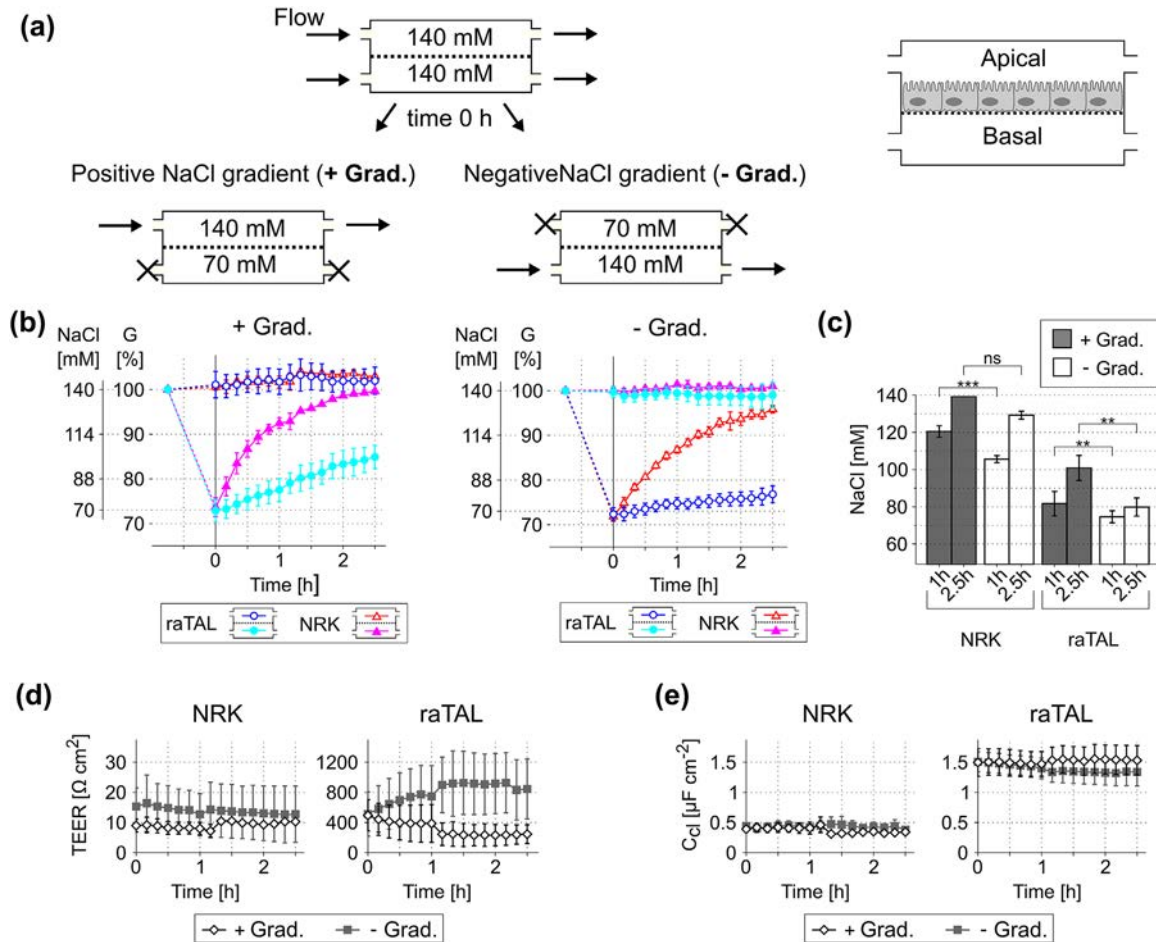
FIGURE 5 Time course of the NaCl concentration during imposed apical to basal positive (apical NaCl > basal NaCl) and negative (apical NaCl < basal NaCl) gradients. (a) Experimental procedure. At time 0, the apical or basal solution containing Ringer's solution of 140 mM of NaCl was replaced by one of 70 mM of NaCl, and the flow was stopped. The opposite compartment was still perfused with Ringer's solution of 140 mM of NaCl. (b) Time course of the electrical conductance at the apical (blue empty circles [raTAL] and red empty triangles [NRK-52E]) and basal (cyan filled circles [raTAL] and magenta filled triangles [NRK-52E]) compartments during positive and negative gradients in raTAL and NRK-52E cells ($n = 4$ except for raTAL cells from 0 to 1 hr ($n = 11$) and for NRK-52E cells from 1 to 2.5 hr ($n = 1$). Data was obtained from two (NRK-52E) and four (raTAL) independent experiments. Conductance was normalized to the data measured at 140 mM of NaCl (100%), and the NaCl concentration was obtained by means of the linear regression line obtained in the electrical characterization. (c) Estimated NaCl concentration at 1 and 2.5 hr after the imposed gradient in both cell types (ns $p > 0.05$; **$p < 0.01$; ***$p < 0.001$ by unpaired student's t-test). Time course of the (d) transepithelial electrical resistance (TEER) and the (e) cell layer capacitance (C_{cl}) during positive (black empty diamonds) and negative (gray filled squares) gradients. TEER differences between positive and negative gradients were $p = 0.90$ at 0 hr; $p = 0.39$ at 1 hr; $p = 0.29$ at 2.5 hr

In addition to the conductance, TEER (Figure 5d) and C_{cl} (Figure 5e) parameters were also measured during both gradient experiments by transepithelial impedance analysis. TEER values for NRK-52E cells at 2.5 hr were 10.3 (+Grad.) and $12.7 \pm 9.3 \, \Omega \, cm^2$ (−Grad.), which are in accordance with low values expected from the PT and with the literature for NRK-52E cells ($12–13 \, \Omega \, cm^2$) (Limonciel et al., 2012; Prozialeck, Edwards, Lamar, & Smith, 2006). For raTAL cells, TEER values were 245 ± 123 (+Grad.) and $844 \pm 397 \, \Omega \, cm^2$ (−Grad.). There are no reported values for this cell line, but TEER for freshly isolated rat medullary TAL tubules is one order of magnitude lower (7,722 Ω cm, corresponding to $48 \, \Omega \, cm^2$ for lumen diameter of 20 μm) (Monzon, Occhipinti, Pignataro, & Garvin, 2017). Interestingly, TEER of raTAL cells increased during the negative gradient and decreased during the positive gradient although not significantly. This

means that ion permeabilities changed to be leakier during the positive gradient and vice versa, which may account for the faster NaCl transport along the positive gradient. The rate of NaCl reabsorption in the TAL segment is dynamic and depends on the luminal NaCl load, that is, cells ceases to reabsorb NaCl when the luminal NaCl concentrations is diluted and if the flow rate is very low, otherwise NaCl reabsorption increases (Greger, 1985). Based on our results, we speculate that raTAL cells might sense ion concentrations on either side and adjust tight junction permeability accordingly. A leaky epithelia would contribute to reabsorb a positive gradient (avoiding salt waste from the body), whereas a tight epithelia would help to maintain the gradient achieved through active transport (which is the normal function in vivo for TAL cells). Unlike TEER, C_{cl} remained unchanged during gradient experiments suggesting that membrane

TABLE 2 Metabolic values during imposed NaCl chemical gradients

	raTAL		NRK	
	Basal (+grad.)	**Apical (−grad.)**	**Basal (+grad.)**	**Apical (−grad.)**
Glucose (mg dl^{-1})	85.2 ± 1.3	$82.3 \pm 1.2^*$	94.3 ± 4.0	$85.0 \pm 2.0^*$
Lactate (mg dl^{-1})	0.15 ± 0.08	$2.65 \pm 1.1^*$	0.23 ± 0.15	$1.5 \pm 0.3^*$
$[Na^+]_o$ (mM)	84.7 ± 1.6	82.0 ± 6.6	$91.0 \pm 3.6^{**}$	90.5 ± 0.5
$[K^+]_o$ (mM)	3.8 ± 0.06	3.8 ± 0.10	4.0 ± 0.21	3.8 ± 0.09
$[Cl^-]_o$ (mM)	88.4 ± 1.6	88.4 ± 3.9	$96.8 \pm 1.7^{**}$	$96.7 \pm 0.9^{**}$
$[Ca^{2+}]_o$ (mM)	3.6 ± 0.06	$3.7 \pm 0.04^*$	3.8 ± 0.06	3.8 ± 0.05
$[Mg^{2+}]_o$ (mM)	2.5 ± 0.07	2.6 ± 0.10	2.6 ± 0.11	2.5 ± 0.07

These values were analyzed from samples collected at the compartment that was initially at 70 mM NaCl (1.5 h) (*$p < 0.05$, apical versus basal; **$p < 0.05$, NRK vs raTAL by unpaired student's t-test) ($n = 3$).

surface areas were maintained. C_{cl} is a lumped element resulting from luminal and basolateral membrane capacitances in series. Its value is approximately $0.5\,\mu F\,cm^{-2}$ for cells with unfolded membranes and increases with the formation of complex surface morphologies. For tubular epithelial cells, which have very particular microvilli and cilium formations, C_{cl} is a useful parameter to electrically differentiate between cell types and to evidence tissue formation and persistence in vitro.

4 | CONCLUSIONS

Monitoring of transepithelial electrical parameters and simultaneous assessment of the ion concentration in real time has been achieved in the presented perfusion chamber using an innovative measurement approach. In particular, both methodologies can be easily combined with an appropriated electrode configuration in microfluidic cell cultures, as it is demonstrated in this work.

Here, we present the feasibility of this methodology for quantifying the concentration of NaCl. Therefore, it is possible the in-line and real-time monitoring of transcellular chemical gradient of NaCl produced by active transporters, which is a primary function of the renal tubule (NaCl reabsorption). In addition, it is essential to integrate sensing capabilities—similar to those of the Ussing chamber—in microphysiological systems that can apply FSS to study renal epithelial cells in a more physiological microenvironment.

ORCID

Jose Yeste iD http://orcid.org/0000-0001-7540-7305

REFERENCES

Benson, K., Cramer, S., & Galla, H.-J. (2013). Impedance-based cell monitoring: Barrier properties and beyond. *Fluids and Barriers of the CNS, 10*, 5.

Brakeman, P., Miao, S., Cheng, J., Lee, C.-Z., Roy, S., Fissell, W. H., & Ferrell, N. (2016). A modular microfluidic bioreactor with improved throughput for evaluation of polarized renal epithelial cells. *Biomicrofluidics, 10*, 064106.

Burg, M. B. (1982). Thick ascending limb of Henle's loop. *Kidney International, 22*, 454–464.

Burg, M. B., & Green, N. (1973). Function of the thick ascending limb of Henle's loop. *The American Journal of Physiology, 224*, 659–668.

Clausen, C., Lewis, S. A., & Diamond, J. M. (1979). Impedance analysis of a tight epithelium using a distributed resistance model. *Biophysical Journal, 26*, 291–317.

Cole, K. S. (1972). *Membranes, ions and impulses: A chapter of classical biophysics*. Berkeley: University of California Press.

Curto,, Curto, V. F., Marchiori, B., Hama, A., Pappa, A.-M., Ferro, M. P., Braendlein, M., . . . Owens, R. M. (2017). Organic transistor platform with integrated microfluidics for in-line multi-parametric in vitro cell monitoring.. *Microsystems & Nanoengineering, 3*, 17028.

Dong, X., Chen, J., He, Q., Yang, Y., & Zhang, W. (2009). Construction of bioartificial renal tubule assist device in vitro and its function of transporting sodium and glucose. *Journal of Huazhong University of Science and Technology [Medical Sciences], 29*, 517–521.

Duan, Y., Weinstein, A. M., Weinbaum, S., & Wang, T. (2010). Shear stress-induced changes of membrane transporter localization and expression in mouse proximal tubule cells. *Proceedings of the National Academy of Sciences, 107*, 21860–21865.

Eng, B., Mukhopadhyay, S., Vio, C. P., Pedraza, P. L., Hao, S., Battula, S., . . . Ferreri, N. R (2007). Characterization of a long-term rat mTAL cell line. *AJP Renal Physiology, 293*, F1413–F1422.

Ferrell,, Ferrell, N., Desai, R. R., Fleischman, A. J., Roy, S., Humes, H. D., & Fissell, WH (2010). A microfluidic bioreactor with integrated transepithelial electrical resistance (TEER) measurement electrodes for evaluation of renal epithelial cells. *Biotechnology and Bioengineering, 107*, 707–716.

Ferrell, N., Ricci, K. B., Groszek, J., Marmerstein, J. T., & Fissell, W. H. (2012). Albumin handling by renal tubular epithelial cells in a microfluidic bioreactor. *Biotechnology and Bioengineering, 109*, 797–803.

FröMter, E., & Diamond, J. (1972). Route of passive ion permeation in epithelia. *Nature New Biology, 235*, 9–13.

Furuse, M., Furuse, K., Sasaki, H., & Tsukita, S. (2001). Conversion of *Zonulae occludentes* from tight to leaky strand type by introducing claudin-2 into madin-darby canine kidney I cells. *The Journal of Cell Biology*, *153*, 263–272.

Gonzalez-Mariscal, L., Contreras, R. G., Bolivar, J. J., Ponce, A., Ramirez, B. C. D., & Cereijido, M. (1990). Role of calcium in tight junction formation between epithelial cells. *American Journal of Physiology—Cell Physiology*, *259*, C978–C986.

Grabias, B. M., & Konstantopoulos, K. (2014). The physical basis of renal fibrosis: Effects of altered hydrodynamic forces on kidney homeostasis. *AJP: Renal Physiology*, *306*, F473–F485.

Greger, R. (1985). Ion transport mechanisms in thick ascending limb of Henle's loop of mammalian nephron. *Physiological Reviews*, *65*, 760–797.

Greger, R. (2000). Physiology of renal sodium transport. *The American Journal of the Medical Sciences*, *319*, 51–62.

Guimerà, A., Gabriel, G., Parramon, D., Calderón, E., & Villa, R. (2009). Portable 4 wire bioimpedance meter with bluetooth link. In O. Dössel, W. C. Schlegel, & R. Magjarevic (Eds.), *World congress on medical physics and biomedical engineering (Munich, DE, 7–12 September 2009)*. (Vol. *25/7*, pp. 868–871). Berlin: Springer.

Ha, L., Jang, K.-J., & Suh, K.-Y. (2014). Chapter 2. Kidney on a chip. In A. Berg, & L. Segerink (Eds.), *RSC nanoscience & nanotechnology*. (pp. 19–39). Cambridge: Royal Society of Chemistry.

Jang, K.-J., Mehr, A. P., Hamilton, G. A., McPartlin, L. A., Chung, S., Suh, K.-Y., & Ingber, D. E. (2013). Human kidney proximal tubule-on-a-chip for drug transport and nephrotoxicity assessment. *Integrative Biology*, *5*, 1119–1129.

Li, H., Sheppard, D. N., & Hug, M. J. (2004). Transepithelial electrical measurements with the Ussing chamber. *Journal of Cystic Fibrosis*, *3*, 123–126.

Limonciel, A., Wilmes, A, Aschauer, L., Radford, R., Bloch, K. M., McMorrow, T., . . . Jennings, P. (2012). Oxidative stress induced by potassium bromate exposure results in altered tight junction protein expression in renal proximal tubule cells. *Archives of Toxicology*, *86*, 1741–1751.

Lorenz, J. N, (2012). Micropuncture of the kidney: A primer on techniques. In R. Terjung (Ed.), *Comprehensive physiology*. (Vol. *2*, pp. 621–637). Hoboken, NJ, USA: John Wiley & Sons, Inc.

Maggiorani, D., Dissard, R., Belloy, M., Saulnier-Blache, J.-S., Casemayou, A., Ducasse, L., . . . Buffin-Meyer, B (2015). Shear stress-induced alteration of epithelial organization in human renal tubular cells. *PLoS ONE*, *10*, e0131416.

Mohammed, S. G., Arjona, F. J., Latta, F., Bindels, R. J. M., Roepman, R., & Hoenderop, J. G. J. (2017). Fluid shear stress increases transepithelial transport of Ca $^{2+}$ in ciliated distal convoluted and connecting tubule cells. *The FASEB Journal*, *31*, 1796–1806.

Monzon, C. M., Occhipinti, R., Pignataro, O. P., & Garvin, J. L. (2017). Nitric oxide reduces paracellular resistance in rat thick ascending limbs by increasing Na $^+$ and Cl $^-$ permeabilities. *American Journal of Physiology-Renal Physiology*, *312*, F1035–F1043.

Muto, S., Hata, M., Taniguchi, J., Tsuruoka, S., Moriwaki, K., Saitou, M., . . . Furuse, M. (2010). Claudin-2–deficient mice are defective in the leaky and cation-selective paracellular permeability properties of renal proximal tubules. *Proceedings of the National Academy of Sciences*, *107*, 8011–8016.

Palmer, L. G., & Schnermann, J. (2015). Integrated control of Na transport along the nephron. *Clinical Journal of the American Society of Nephrology*, *10*, 676–687.

Planelles, G. (2004). Chloride transport in the renal proximal tubule. *Pflügers Archiv—European Journal of Physiology*, *448*, 561–570.

Prozialeck, W. C., Edwards, J. R., Lamar, P. C., & Smith, C. S. (2006). Epithelial barrier characteristics and expression of cell adhesion molecules in proximal tubule-derived cell lines commonly used for in vitro toxicity studies. *Toxicology in Vitro*, *20*, 942–953.

Raghavan, V., Rbaibi, Y., Pastor-Soler, N. M., Carattino, M. D., & Weisz, O. A. (2014). Shear stress-dependent regulation of apical endocytosis in renal proximal tubule cells mediated by primary cilia. *Proceedings of the National Academy of Sciences*, *111*, 8506–8511.

Robbins, J. (1972). *Ions in solution 2: An introduction to electrochemistry*. Oxford: Oxford University Press.

Stockand, J. D, Vallon, V., & Ortiz, P. (2012). In vivo and ex vivo analysis of tubule function. In R. Terjung (Ed.), *Comprehensive physiology*. (Vol. *2*, pp. 2495–2525). Hoboken, NJ, USA: John Wiley & Sons, Inc.

Taub, M., & Sato, G. (1980). Growth of functional primary cultures of kidney epithelial cells in defined medium. *Journal of Cellular Physiology*, *105*, 369–378.

Terryn, S., Jouret, F., Vandenabeele, F., Smolders, I., Moreels, M., Devuyst, O., . . . Kerkhove, E. V. (2007). A primary culture of mouse proximal tubular cells, established on collagen-coated membranes. *AJP: Renal Physiology*, *293*, F476–F485.

Ussing, H. H., & Zerahn, K. (1951). Active transport of sodium as the source of electric current in the short-circuited isolated frog skin. *Acta Physiologica Scandinavica*, *23*, 110–127.

Wang, X.-B., Huang, Y., Gascoyne, P. R. C., Becker, F. F., Hölzel, R., & Pethig, R. (1994). Changes in Friend murine erythroleukaemia cell membranes during induced differentiation determined by electrorotation. *Biochimica et Biophysica Acta (BBA)—Biomembranes*, *1193*, 330–344.

Wegener, J., Abrams, D., Willenbrink, W., Galla, H.-J., & Janshoff, A. (2004). Automated multi-well device to measure transepithelial electrical resistances under physiological conditions. *BioTechniques*, *37*, 590, 592–594.

Weinbaum, S., Duan, Y., Satlin, L. M., Wang, T., & Weinstein, A. M. (2010). Mechanotransduction in the renal tubule. *AJP: Renal Physiology*, *299*, F1220–F1236.

Yeste, J., Illa, X., Guimerà, A., & Villa, R. (2015). A novel strategy to monitor microfluidic in-vitro blood-brain barrier models using impedance spectroscopy. In S. van den Driesche (Ed.), *Bio-MEMS and medical microdevices II (Barcelona, ES, 4–6 may 2015)*. (p. 95180N). Bellingham, WA: SPIE.

Yeste, J., Illa, X., Gutiérrez, C., Solé, M., Guimerà, A., & Villa, R. (2016). Geometric correction factor for transepithelial electrical resistance measurements in transwell and microfluidic cell cultures. *Journal of Physics D: Applied Physics*, *49*, 375401.

Yu, A. S. L., Enck, A. H., Lencer, W. I., & Schneeberger, E. E. (2003). Claudin-8 expression in madin-darby canine kidney cells augments the paracellular barrier to cation permeation. *Journal of Biological Chemistry*, *278*, 17350–17359.

SUPPORTING INFORMATION

Additional Supporting Information may be found online in the supporting information tab for this article.

How to cite this article: Yeste J, Martínez-Gimeno L, Illa X, et al. A perfusion chamber for monitoring transepithelial NaCl transport in an in vitro model of the renal tubule. *Biotechnology and Bioengineering*. 2018;1–10. https://doi.org/10.1002/bit.26574